

# Questions on the solar structure and evolution

Sergey V. Ayukov • Vladimir A. Baturin

© Springer-Verlag ••••

**Abstract** While term "standard solar model" is commonly established now, several questions still need to be clarified. First problem is a contradiction between the recent observational indications on low  $Z$  and difficulties in computing of a helioseismic model with these abundances. We present and discuss the solar model with differential  $Z$  changes, i.e. varying specific element abundances what is allowed by using SAHA-S EOS and OPAL opacities. The model can be in better agreement with helioseismic inversions for the adiabatic exponent in solar convective zone. Second problem is connected with the bottom of the convection zone and the boundary of convective mixing. Conditions at the mixing boundary determine the rate of helium settling from the convection zone and therefore affect the whole element distribution in the Sun. And taking into account penetrating convection may lead to change in solar evolution, what is illustrated with our evolutionary calculations.

**Keywords** Sun; opacity; equation of state; abundances

## 1 Introduction

The modern model of the internal structure of the Sun is a product of many components. One must mix plasma physics, structure equations and observational data and then solve. Solution is numerical. The result can be compared to the real Sun in many ways, one of them is helioseismic inversions. Helioseismic inversions are data obtained by analyzing solar oscillation frequencies. In this article surface helium abundance,

convection zone depth and sound speed profile are used as inversion data (Basu & Antia (2008)).

One of the first very good agreements between model and inversions has been achieved about 13 years ago when Model S of Christensen-Dalsgaard (Christensen-Dalsgaard et al. (1996)) was calculated and published. Figure 1 displays sound speed differences between models and inversion. Original Model S was computed with OPAL92 opacities (Rogers, Iglesias (1992)). Later there was a version of Model S with updated opacity tables, OPAL95 (Iglesias, Rogers (1996)). Two our models are also plotted here. One is more or less similar to Model S with OPAL95 opacities (720-0111) and another is with updated physics but the same abundances as in Model S (720-0100). While difference between models do exist, the general agreement between models is remarkable. This indicates that nothing bad has happened to model physics during 13 years, at least in our interpretation. Except abundances of course.

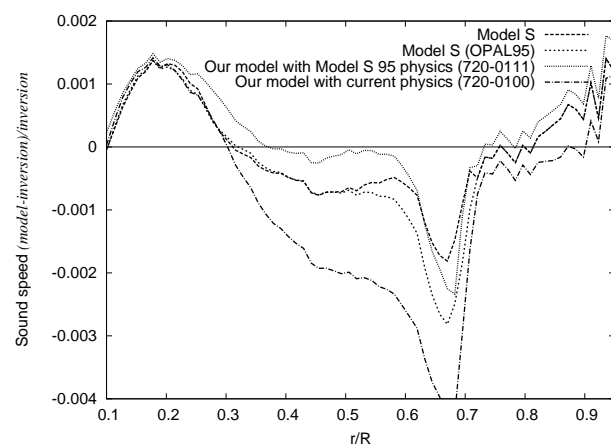


**Fig. 1** Sound speed comparison between models and inversion Basu & Antia (2008)

An important input for solar modelling is a set of relative abundances of elements heavier than helium. Such set is usually called a ‘mixture’. One of the mixture’s characteristics is  $Z/X$  (heavy elements to hydrogen) ratio. For quite long time  $Z/X$  was assumed to be about 0.02-0.025 (AG89 Anders & Grevessee (1989), GN93 Grevesse, Noels (1993), GS98 Grevesse, Sauval (1998)), and all model calculations relied on this value. In 2004 new and advanced 3D models were used to compute solar atmosphere and from these models came new relative abundance values (Asplund et al. (2004)). According AGS05 (Asplund et al. (2005)) the amount of elements heavier than helium is significantly lower than was assumed by previous works (GN93, GS98), 0.0165 versus 0.0245. Models computed with  $Z/X = 0.0165$  exhibit much large differences against inversion results (e.g, recent review Basu & Antia (2008)). This is a still unsolved controversy in the solar modelling.

## 2 Model physics

Besides chemical composition, main physics factors affecting model of the Sun are opacity, equation of state, nuclear reaction rates, element diffusion and convective energy transfer. Since this works concentrates on chemical composition and related issues, special care was taken to ensure proper treatment of complex chemical composition in these factors.

The most complex issue is opacity. It is also a factor which strongly depends on heavy element abundances. To compute model properly we have developed interpolation scheme which allows to interpolate OPAL opacities by 20 elements: hydrogen plus 19 heavy elements. Source tables were provided by Lawrence Livermore Laboratory<sup>1</sup>; they are supplemented by Ferguson et al. (2005) low-temperature tables with fixed mixture. Interpolation scheme includes the following subtables, each providing opacity values for range of temperature, density and hydrogen content: a) opacity for  $Z = 0.01$ , standard GN93 mixture; b) 18 opacity derivatives by every element while keeping total  $Z = 0.01$ ; c) opacity for  $Z = 0.02$ , standard GN93 mixture; d) 18 opacity derivatives by every element while keeping total  $Z = 0.02$ . Note that 18 derivatives are used since 19th derivative is linearly dependent on the rest (total  $Z$  is constant). Derivatives are computed numerically from the set of source tables obtained at Lawrence Livermore website. This scheme allows to obtain opacity for arbitrary mixture of H and 19 heavy elements. Its precision was not studied in detail however.

Almost all models presented in this work use SAHA-S equation of state (Gryaznov et al. (2004)). It is in tabulated form and can be interpolated by  $T$ ,  $\rho$ ,  $X$  and mass fractions of CNO, Ne and Fe/Si.

## 3 Sun calibration and abundances

To compute model of the Sun is to calculate model which has proper values of radius and luminosity. One varies initial hydrogen content  $X_0$  and convection parameter  $\alpha$  to adjust radius and luminosity. This process is often called ‘calibration’; model becomes ‘calibrated’ with  $L = L_{\odot}$  and  $R = R_{\odot}$ . In this typical scheme  $Z/X$  ratio does not participate in calibration. However if model is computed with specific mixture it must have predetermined heavy element abundances at the outer layers at the solar age. When element settling is not taken into account  $Z/X$  does not change between ZAMS and current Sun, but when diffusion is in effect, achieving given  $Z/X$  in the current Sun becomes a problem.

Our solution is to use third calibration parameter. Besides  $X_0$  and  $\alpha$ ,  $Z_0$  (initial heavy element abundance) is also varied to get correct values of  $R$ ,  $L$ ,  $Z/X$  at the solar age. This approach still has internal inconsistency as abundances of different elements are altered differently by diffusion, but this is second order error, or at least we believe it to be so. In other words, all our models with specific mixture are calibrated to exact value of  $Z/X$  which is specific to given mixture.  $Z/X$  can be computed from relative numeric abundances of the given mixture. The partial derivatives for calibration are in Table 1.

**Table 2** Calibration derivatives

|        | $L$     | $R$    | $Z/X$    |
|--------|---------|--------|----------|
| $d/dA$ | 0.0279  | -0.094 | 0.0006   |
| $d/dX$ | -8.158  | -2.003 | -0.01297 |
| $d/dZ$ | -41.701 | -8.807 | 1.368    |

If calibration does not converge after 10 iterations, these derivatives are recomputed for specific model which is being calibrated. Default calibration precision for  $R$  and  $L$  is  $10^{-8}$ .

## 4 Element diffusion

While effect element diffusion on the solar evolution was extensively studied, this work adds a new dimension: per-element diffusion treatment. Since diffusion rate depends on ion mass and charge (we’re using Michaud,

<sup>1</sup><http://adg.llnl.gov/Research/OPAL/new.html>

| Model    | $Y_{surf}$ | $Z_{surf}$ | $Z/X_{surf}$ | $R_{cz}$              | Note                                        |
|----------|------------|------------|--------------|-----------------------|---------------------------------------------|
| 720-0100 | 0.24147    | 0.018073   | 0.02441      | 0.71466               | GN93 mixture                                |
| 720-0101 | 0.24157    | 0.018071   | 0.02441      | 0.71447*              | overshooting regime 1                       |
| 720-0102 | 0.24158    | 0.018071   | 0.02441      | 0.71496               | diffusion rates by oxygen (see sect. 5)     |
| 720-0103 | 0.24291    | 0.018039   | 0.02441      | 0.71673               | partial ionization simulation (see sect. 5) |
| 720-0105 | 0.24074    | 0.018091   | 0.02441      | 0.71423               | OPAL1996 EOS                                |
| 720-0106 | 0.22905    | 0.013136   | 0.01733      | 0.72661               | AGS05, Ne +0.2                              |
| 720-0107 | 0.24172    | 0.017099   | 0.02307      | 0.71795               | GS98 mixture                                |
| 720-0108 | 0.22587    | 0.012583   | 0.01652      | 0.73023               | AGS05 mixture                               |
| 720-0109 | 0.24188    | 0.02441    | 0.71146*     | overshooting regime 2 |                                             |
| 720-0110 | 0.24163    | 0.018070   | 0.02441      | 0.71443*              | overshooting regime 4                       |
| 720-0111 | 0.24156    | 0.018072   | 0.02441      | 0.71210               | physics as in Model S                       |
| 720-0113 | 0.22382    | 0.012232   | 0.01601      | 0.73256               | AGS05, Ne -0.2                              |
| 720-0114 | 0.23388    | 0.014003   | 0.01862      | 0.72100               | AGS05, Ne +0.4                              |
| 720-0115 | 0.25260    | 0.019939   | 0.02741      | 0.70760               | AG89 mixture                                |
| 720-0116 | 0.24108    | 0.018083   | 0.02441      | 0.71392               | OPAL2005 EOS                                |
| 720-0117 | 0.24114    | 0.018081   | 0.02441      | 0.71411               | OPAL2001 EOS                                |
| 720-0118 | 0.23715    | 0.014605   | 0.01952      | 0.71717               | AGS05, Ne +0.5                              |
| 720-0119 | 0.24143    | 0.018075   | 0.02441      | 0.71429               | mixing near lower CZ boundary               |
| 720-0120 | 0.24113    | 0.015356   | 0.02065      | 0.71239               | AGS05, Ne +0.6                              |

**Table 1** Model surface chemical composition and convection zone boundary position. All models are computed with GN93 mixture, SAHA-S equation of state, OPAL 19-component opacity except otherwise specified. \*Convection zone boundary does not exist in models with overshooting. Data indicate Schwarzschild criterion location

Proffitt (1993) formulation) different elements settle at different rates.

Three models are plotted on Figure 2. 720-0100 is our full model which includes separate diffusion treatment for 20 elements (helium and 19 metals, fully ionized), 720-0102 is usual approach when all elements diffuse at the rate of oxygen. 720-0103 represents an attempt to estimate significance of partial ionization; diffusion rates for elements heavier than Ne were computed assuming 50% ionization. Plot indicates that effects considered are small and in general needn't have to be taken into account. Nevertheless all our models (except when specified) are computed with per-element diffusion treatment.

Turcotte et al. (1998) have computed similar models, though our computations take into account effect of abundance profile changes on the equation of state. It was also found that effect of detailed diffusion treatment is not significant.

## 5 Convective overshooting

Strict adherence to Schwarzschild criterion produces sharp detail in the temperature gradient at the lower convection zone boundary. It is unlikely that real Sun is properly described by such model; however, the adequate formalism for transition from convection to radiative energy transfer is absent. We present several

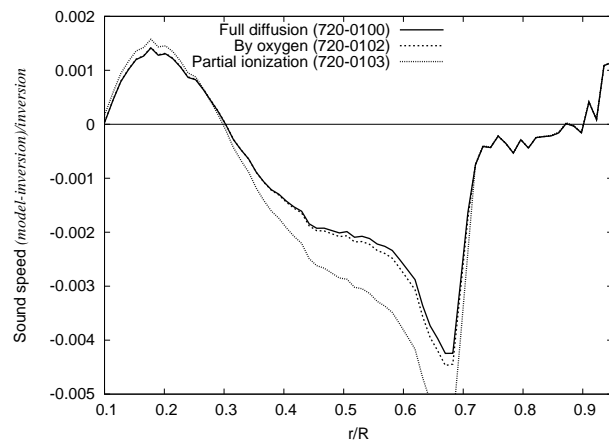


**Fig. 2** Effect of 19-element diffusion calculations and partial ionization; see explanation in text

models ('regimes') which illustrate possible ways to describe this transition region. Corresponding temperature gradient profiles are displayed on Figure 3. Regime 1 is 'convective elements are slowing down before hitting the radiative zone', regime 4 is 'shooting over the boundary' (Shaviv & Salpeter (1973)) and regime 2 is similar to 1 but very intensive. Regime 4 looks like real overshooting, in other words convective gradient extends into nonconvective area. Unlike it, regimes 1 and 2 also touch convective zone; convection elements

are slowed down before the boundary. Regime 2 is probably too extreme.

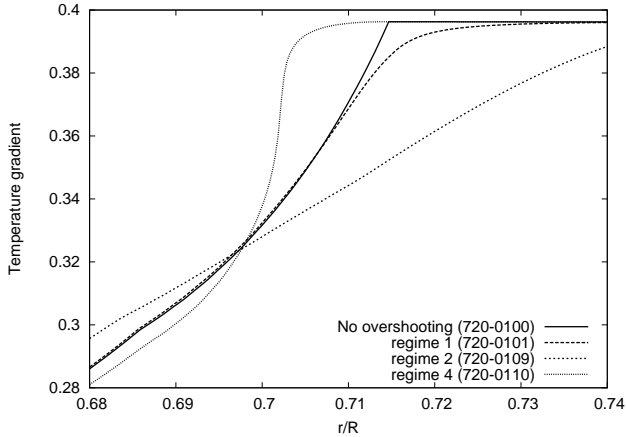


**Fig. 3** Overshooting, temperature gradient

In all cases overshooting changes the definition of ‘the boundary of the convection zone’ term. Effectively these models do not have the characteristic usually called convection zone depth, but this does not prevent from analyzing sound speed profile (Figure 4).

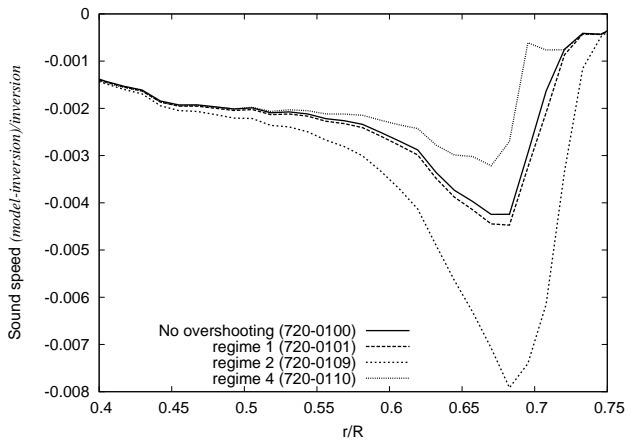


**Fig. 4** Overshooting, effect on sound speed profile

The main effect on sound speed is of course the effective change in convection zone depth. Regime 4 effectively enlarges convection zone and its depth becomes closer to what is assumed by inverted sound speed.

Another consequence of overshooting is change in the chemical composition near the boundary of the convection zone (‘overmixing’). Only one model was implemented, a simple smoothing. Due to space constraints no plot is presented here, but effect on sound speed profile is very small. Effect on Brunt-Vaisala frequency  $N^2$  is more prominent because it depends on density derivatives and in turn on chemical composition derivatives.

Model with overmixing has nonzero  $N^2$  in the lower layers of the convection zone.

## 6 Neon abundance and importance of equation of state

Noble gases on the Sun do not form spectral lines suitable for analysis and they escape from meteorites, so all abundance determinations are indirect. Most mixtures published before XXI century assumed rather stable neon abundance, but AGS05 result has lowered it by 0.2 dex. Bahcall et al. (2005) have shown that low-Z problem can be solved with neon abundance increase, though they have also changed other elements. We have computed several models with different neon abundance. One model has even less neon than AGS05 and four are neon-enriched. All other elements are at their AGS05 abundances.

The effect on sound speed profile is rather straightforward (Figure 5) and looks to be mostly caused by convection zone depth change. The model with 0.5 increase has convection zone boundary at 0.717 vs. AGS05 model with convection zone boundary at 0.730. Increasing neon abundances does reduce discrepancy, but required 0.5 dex increase looks unrealistic.

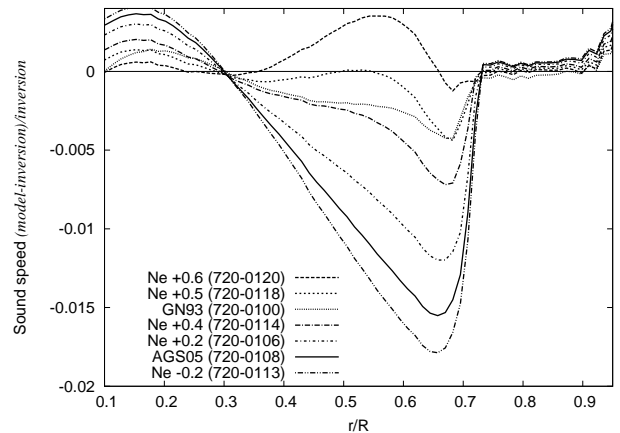


**Fig. 5** Ne abundance and sound speed comparison

Besides sound speed profile (largely affected by opacity) there’s adiabatic exponent  $\Gamma_1$  issue (Figure 6, made possible by SAHA-S EOS tables which can be interpolated by Ne abundance). Neon produces prominent detail on the  $\Gamma_1$  profile around 500 000K. If high-precision  $\Gamma_1$  inversion is available it could be used to estimate neon abundance in the convection zone.

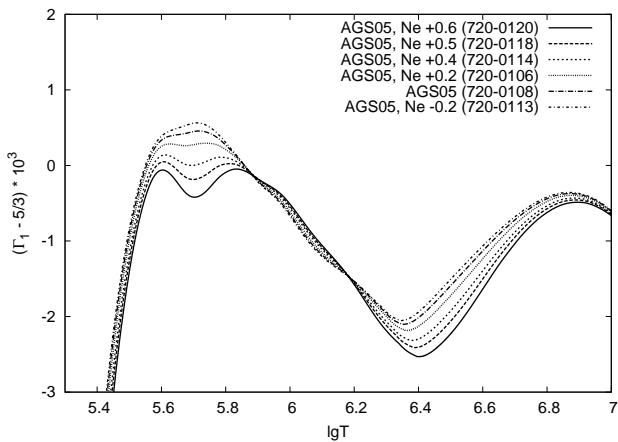


**Fig. 6** Ne abundance and adiabatic exponent

## 7 Conclusion

Figure 7 displays a map in the land of helium content and convection zone depth. The black rectangle is current inversion data (Basu & Antia (2008)). For models with overshooting we don't really know what convection zone depth to assign, but these models aren't plotted here. The most prominent feature is that almost all models lie on the straight band. We suggest the following explanation for this behaviour. Abundances affect opacity and convection zone depth. Convection zone boundary position determines the diffusion flow rate of helium from the convection zone, and this difference in the flow rate causes difference in surface helium abundance.

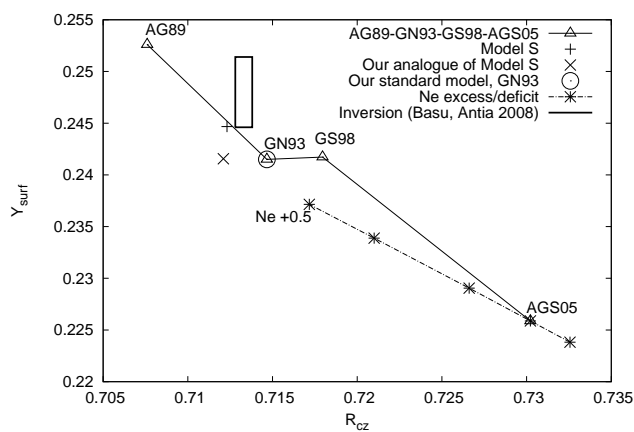


**Fig. 7** Helium–convection zone depth roadmap

There have been many attempts to solve low- $Z$  controversy. In this work it is shown that increasing Ne by 0.5 dex solves the problem, but in this model neon constitutes over 26% (by mass) of all heavy elements. Unfortunately direct measurements of Ne/Ar abundances

on the Sun cannot be performed, but neon abundance can in principle be inferred from adiabatic exponent  $\Gamma_1$  profile.

## 8 Acknowledgements

This work was supported by ISTC grant 3755.

## References

- Basu, S., Antia H.M.: Physics Reports 457, 217 (2008)  
 Christensen-Dalsgaard, J. et al.: Science, 272, 1286 (1996)  
 Rogers, F.J., Iglesias, C.A.: Astrophys. J. Suppl. Ser. 79, 507 (1992)  
 Iglesias, C.A., Rogers, F.J.: Astrophys. J., 464, 943 (1996)  
 Anders, E., Grevesse, N.: Geochimica et Cosmochimica Acta 53, 197 (1989) AG89  
 Grevesse, N., Noels, A.: In: Prantzos, N., Vangioni-Flam, E., Cass'è, M. (Eds.), Origin and Evolution of the Elements. Cambridge Univ. Press (1993) GN93  
 Grevesse, N., Sauval, A.J.: Space Sci. Rev. 85, 161 (1998) GS98  
 Asplund, M., Grevesse, N., Sauval, A.J., Allende Prieto, C., Kiselman, D.: Astron. Astrophys., 417, 751 (2004)  
 Asplund, M., Grevesse, N., Sauval, A.J.: In: Barnes, T.G., Bash, F.N. (Eds.), Cosmic Abundances as Records of Stellar Evolution and Nucleosynthesis. ASP Conf. Ser., 336, 25 (2005) AGS05  
 Ferguson, J.W., Alexander, D.R., Allard, F., Barman, T., Bodmarik, J.G., Hauschildt, P.H., Heffner-Wong, A., Tamanai, A.: Astrophys. J. 623, 585 (2005)  
 Gryaznov V.K., Ayukov S.V., Baturin V.A., Iosilevskiy I.L., Starostin A.N., Fortov V.E.: In: Equation-of-State and Phase-Transition Issues in Models of Ordinary Astrophysical Matter, Eds. V.Celebonovic, W.Dappen, D.Gough. AIP Conference Proceedings, 731, New York, 147 (2004)  
 Michaud, G., Proffitt, C.R.: In: Inside the stars, IAU Colloquium 137, ASP Conference Series 40, Eds. W.W.Weiss and A.Baglin, New York, 137 (1993)  
 Turcotte, S., Richer, J., Michaud, G., Iglesias, C.A., Rogers, F.J.: Astrophys. J., 504, 539 (1998)  
 Shaviv, G., Salpeter, E.E.: Astrophys. J., 184, 191 (1973)  
 Bahcall, J.N., Basu, S., Serenelli, A.M.: Astrophys. J., 631, 1281 (2005)